Journal of Scientific Computing (2018) 77:1468–1489
https://doi.org/10.1007/s10915-018-0862-z

Enriched Spectral Methods and Applications to Problems with Weakly Singular Solutions

Sheng Chen[1,2] · **Jie Shen**[3,4]

Received: 4 February 2018 / Revised: 17 September 2018 / Accepted: 11 October 2018 /
Published online: 30 October 2018

Abstract
Usual spectral methods are very effective for problems with smooth solutions, but their accuracy will be severely limited if solution of the underlying problems exhibits singular behavior. We develop in this paper enriched spectral-Galerkin methods (ESG) to deal with a class of problems for which the form of leading singular solutions can be determined. Several strategies are developed to overcome the ill conditioning due to the addition of singular functions as basis functions, and to efficiently solve the approximate solution in the enriched space. We validate ESG by solving a variety of elliptic problems with weakly singular solutions.

Keywords Weakly singular solution · Spectral-Galerkin method · Enriched space · Jacobi polynomials · Error estimate

Mathematics Subject Classification 65N35 · 41A10 · 41A30 · 41A99

Dedicated to Bernardo Cockburn on the occasion of his 60th birthday.

Sheng Chen is partially supported by the Foundation of Jiangsu Normal University (Grant No. 17XLR013), the Natural Science Foundation of the Jiangsu Higher Education Institutions of China (Grant No. BK20181002), the National Natural Science Foundation for the Youth of China (Grant No. 11801235) and the Postdoctoral Science Foundation of China (Grant No. BX20180032). Jie Shen is partially supported by NSF Grants DMS-1620262, DMS-1720442 and AFOSR Grant FA9550-16-1-0102.

✉ Jie Shen
shen7@purdue.edu

1 School of Mathematics and Statistics, Jiangsu Normal University, Xuzhou 221116, People's Republic of China

2 Beijing Computational Science Research Center, Beijing 100193, People's Republic of China

3 Department of Mathematics, Purdue University, West Lafayette, IN 47907-1957, USA

4 School of Mathematical Sciences and Fujian Provincial Key Laboratory on Mathematical Modeling and High Performance Scientific Computing, Xiamen University, Xiamen 361005, Fujian, People's Republic of China

1 Introduction

Spectral methods are capable of providing highly accurate solutions to smooth problems with significantly less unknowns than using a finite-element or finite difference methods [7,9,16,34]. However, solutions to many problems of interest exhibit singular behaviors, such as those caused by domain corners or points where boundary condition changes type or fractional derivatives. For these problems, usual spectral methods based on orthogonal polynomials/functions does not yield satisfactory convergence rate.

Within the finite element framework, many different methods are developed to deal with problems with singular solutions. They can be roughly classified into two categories: (i) one is based on local adaptivity [26]; and (ii) the other is the so called singular functions method [37] and its generalized version *extended or generalized finite element method* (GFEM/XFEM) (cf. [3,14] and the references therein) in which one adds, to the usual local polynomial basis, special shape functions or local singular functions that capture local singular properties of the underlying problem. However, there appears to be no systematical framework in the context of spectral methods available to deal with problems with singular solutions. In [31], a spectral-tau method was used to deal with the singularity of the 2-D Stokes equations in a rectangular domain. In [2,6,30], the authors subtracted the strongest singular function from the solution to improve the accuracy of spectral methods for Stokes and Navier–Stokes equations. Recently in [35], a Müntz spectral method is introduced to deal with a class of problems which admit a singular expansion of the Müntz type. In [11,23,24,39], different kind of generalized Jacobi polynomials/functions are used to deal with singularities in fractional differential equations.

In this paper, we shall develop enriched spectral Galerkin methods (ESG) which is in the same spirit of extended or generalized finite element method by adding singular functions to the usual bases. But unlike in GFEM/XFEM, we shall add global singular functions to the existing basis functions. However, there are some essential difficulties that we need to overcome for ESG to work efficiently and accurately. First, the singular functions usually do not satisfy the underlying boundary conditions so a Galerkin approach can not be directly applied. Second, the singular functions are not orthogonal functions, and adding them to the bases leads to very ill conditioned linear system that is (i) difficult to solve, and (ii) its accuracy can be severely affected by the ill conditioning. We shall develop several effective strategies in the next section to deal with these issues. In particular, based on the particular fact that a spectral approximation for the smooth part of the solution will converge very fast, an innovative approach (referred as ESG-II) is proposed to approximately solve the linear system in ESG.

The remainder of the paper is organized as follows. In the next section, we develop a general framework for the enriched spectral-Galerkin methods. Two different solvers are proposed: one solves the ESG system using the Schur-complement approach, the other is an approximate solver which is more efficient and less prone to the ill conditioning. Two 1-D applications are considered to validate ESG-I and ESG-II. In Sect. 3, we consider Poisson equations in various contexts. We first identify leading singular solutions, and then apply ESG to obtain accurate solutions. A nonlinear problem is considered as well. In Sect. 4, we study an 1-D fractional differential equation, deriving the form of its singular solutions and then apply ESG to obtain accurate solutions. Some concluding remarks are given in Sect. 5.

2 Enriched Spectral-Galerkin Methods (ESG)

To fix the idea, we consider the following weak formulation of an elliptic problem: Given $f \in X'$, find $u \in X$ such that

$$a(u, v) =< f, v >, \quad \forall\, v \in X, \tag{2.1}$$

where X is a Hilbert space with norm $\|\cdot\|_X$ and X' is its dual space, $a(u, v)$ is a coercive and continuous bilinear form in $X \times X$, i.e., there exist $\alpha, \beta > 0$ such that

$$\alpha\|u\|_X^2 \le a(u, u), \qquad a(u, v) \le \beta\|u\|_X\|v\|_X, \qquad \forall\, u, v \in X. \tag{2.2}$$

Let $X_N := \text{span}\{\phi_n\}_{n=1}^N$ with $\phi_n \in X$ being certain global polynomials/functions such that $X_N \to X$. Then, the classical spectral-Galerkin method is to find $u_N \in X_N$ such that

$$a(u_N, v_N) =< f, v_N >, \quad \forall\, v_N \in X_N. \tag{2.3}$$

If the solution u of the problem (2.1) is smooth, then $\|u_N - u\|_X$ will rapidly converge to zero. However, in many situations, the solution will not be smooth due to various facts such as corner singularities, non-matching boundary conditions, non-smooth coefficients, so the classical spectral-Galerkin method with usual basis functions will not lead to accurate approximate solution.

For many problems with non-smooth solutions due to corner singularities, non-matching boundary conditions or fractional derivatives, it is possible to determine the forms of a few leading singular terms. Assuming that the k first leading singular terms are $\psi_i,\ i = 1, 2, \ldots, k$, it is then natural to add those singular terms to the approximation space X_N, leading to the so called enriched spectral method. While similar ideas have been frequently used in the context of finite elements (cf. [3,14] and the references therein), very few attempts have been made in the context of spectral methods. One difficulty in the practical implementation of enriched spectral method is that the singular functions usually do not satisfy the underlying boundary condition, i.e., they do not belong to the solution space X. To overcome this difficulty the authors of [31] used a spectral-tau method where the test functions are simply polynomials while singular functions are included in the trial space. Although this leads to a square linear system, it is not clear whether it is well posed and it leads to a very ill conditioned system that is difficult and expensive to solve.

To construct a more efficient and accurate enriched spectral method, we shall pre-process the singular functions $\{\psi_i\}$ as follows:

- First, in order to use a spectral-Galerkin approach instead of the spectral-tau method, we modify the singular functions so that they satisfy the underlying homogeneous boundary conditions. We shall explain this process with the following example:

$$b(x)u - \nabla\cdot(a(x)\nabla u) = f \quad x \in \Omega := (-1, 1)^d; \quad u|_{\partial\Omega} = 0. \tag{2.4}$$

  Given a (weakly) singular function $\psi \in C(\bar{\Omega})$.

  - $d = 1$: we set $\phi = \frac{1+x}{2}\psi(1) + \frac{1-x}{2}\psi(-1)$. Setting $\hat{\psi}(x) = \psi(x) - \phi(x)$, then the modified singular function satisfies $\hat{\psi}(\pm 1) = 0$.
  - $d > 1$: Let Σ_N be the set of spectral collocation points on $\partial\Omega$. For $d = 2$, a detailed procedure is given in [32] for constructing a simple polynomial ϕ such that $\phi|_{\Sigma_N} = \psi|_{\Sigma_N}$. Setting $\hat{\psi}(x) = \psi(x) - \phi(x)$, then the modified singular function satisfies $\hat{\psi}\big|_{\Sigma_N} = 0$. This procedure can be extended to $d \ge 3$.

- Second, in order to alleviate the ill conditioning, we use the modified Gram–Schimdt process [5] to determine a set of orthogonal functions $\{\tilde{\psi}_j\}_{j=1}^k$ which span the same space as $\{\hat{\psi}_j\}_{j=1}^k$.

Therefore, given a set of singular functions, $\psi_i,\ i = 1, 2, \ldots, k$, for the problem (2.1), let $\tilde{\psi}_i$ $(i = 1, 2, \ldots, k)$ be the modified singular functions as described above and denote $S_k := \text{span}\{\tilde{\psi}_i\}_{i=1}^k$. We shall then look for approximation in the enriched space

$$X_N^k := X_N \oplus S_k. \tag{2.5}$$

2.1 ESG-I. Standard Galerkin Approach

The standard Galerkin method applied to the enriched space is: Find $u_N^k \in X_N^k$ s.t.

$$a(u_N^k, v_N^k) =< f, v_N^k >, \quad \forall\, v_N^k \in X_N^k. \tag{2.6}$$

Thanks to (2.2), we have immediately the following error estimate for (2.6):

$$\|u - u_N^k\|_X \lesssim \inf_{v \in X_N^k} \|u - v\|_X. \tag{2.7}$$

Thus, the theoretical convergence rate of $u - u_N^k$ will improve significantly, as k increases, over that of $u - u_N$, with u_N being the solution of (2.3). We recall that, in many cases, the linear system associated to (2.3) can be efficiently solved by choosing suitable orthogonal basis functions [32,34]. However, since $\mathcal{S}_k$ and X_N are two sets consisting of very different functions and that $\{\psi_i\}$ are not orthogonal and often behave similarly away from singularity, the linear system associated with (2.6) are very ill conditioned and can not be efficiently solved by direct inversion.

Since the linear system for (2.3) in X_N can be efficiently solved, and k is usually a very small number, we can solve the linear system for (2.6) in X_N^k using the Schur-complement approach as follows.

Let $X_N = \text{span}\{\phi_n : n = 1, 2, \ldots, N\}$. We write $u_N^k = \sum_{j=1}^N \tilde{u}_j \phi_j + \sum_{j=1}^k \tilde{s}_j \tilde{\psi}_j$. Splitting the unknown into two parts $\vec{\mathbf{u}} = (\tilde{u}_1\ \tilde{u}_2\ \ldots\ \tilde{u}_N)^T$ and $\vec{\mathbf{s}} = (\tilde{s}_1\ \tilde{s}_2\ \ldots\ \tilde{s}_k)^T$, and taking $v_N^k = \phi_n,\ n = 1, 2, \ldots, N$ and $\tilde{\psi}_i,\ i = 1, 2, \ldots, k$ in (2.6), we obtain the following linear system:

$$\mathbf{M}\vec{\mathbf{U}} := \begin{bmatrix} \mathbf{A} & \mathbf{B} \\ \mathbf{C} & \mathbf{D} \end{bmatrix} \begin{bmatrix} \vec{\mathbf{u}} \\ \vec{\mathbf{s}} \end{bmatrix} = \begin{bmatrix} \vec{\mathbf{f}} \\ \vec{\mathbf{f}}^s \end{bmatrix}, \tag{2.8}$$

where

$$\begin{array}{llll} \mathbf{A} = (a_{nm})_{N\times N}, & \mathbf{D} = (d_{ij})_{k\times k}, & a_{nm} = a(\phi_m, \phi_n), & d_{ij} = a(\tilde{\psi}_j, \tilde{\psi}_i), \\ \mathbf{B} = (b_{ni})_{N\times k}, & \mathbf{C} = (c_{in})_{k\times N}, & b_{ni} = a(\tilde{\psi}_i, \phi_n), & c_{in} = a(\phi_n, \tilde{\psi}_i), \\ \vec{\mathbf{f}} = (f_n)_{N\times 1}, & \vec{\mathbf{f}}^s = (f_i^s)_{k\times 1}, & f_n = (f, \phi_n), & f_i^s = (f, \tilde{\psi}_i). \end{array} \tag{2.9}$$

Remark 2.1 The computation of the entries involving singular terms $\tilde{\Psi}_i$ needs special care. Fortunately, many singular terms behave like Jacobi weight $(1-x)^a(1+x)^b$, so these integrals can be computed accurately using the corresponding Jacobi–Gauss quadrature formula. For other type of singular functions, e.g. log functions, we can still compute them to required accuracy using a Gauss quadrature with suitably more points than the number of unknowns. □

The above system can be efficiently solved by forming the Schur-complement matrix $\mathbf{CA}^{-1}\mathbf{B} - \mathbf{D}$, and then we can obtain $\vec{\mathbf{s}}$ and $\vec{\mathbf{u}}$ successively from

$$(\mathbf{CA}^{-1}\mathbf{B} - \mathbf{D})\,\vec{\mathbf{s}} = \mathbf{CA}^{-1}\vec{\mathbf{f}} - \vec{\mathbf{f}}^{s}, \quad \mathbf{A}\vec{\mathbf{u}} = \vec{\mathbf{f}} - \mathbf{B}\vec{\mathbf{s}}. \tag{2.10}$$

Note that $\mathbf{A}$ is the matrix for the classical spectral-Galerkin method in X_N, so the system

$$\mathbf{A}\vec{\mathbf{x}} = \vec{\mathbf{g}} \tag{2.11}$$

can usually be solved very efficiently. The formation of the Schur-complement requires solving (2.11) k times. Then we can obtain $\vec{\mathbf{s}}$ and $\vec{\mathbf{u}}$ from (2.10) by solving one $k \times k$ linear system and one more (2.11). Hence, the total cost of this algorithm is essentially $(k + 1)$ solvers of (2.11), which is very efficient assuming (2.11) can be solved fast.

While the above approach is very efficient, and alleviates, to some extent, the ill conditioning problem caused by singular functions, the numerical results can still be plagued by ill conditioning as k increases, see the left of Fig. 1, where we observe that the error do not decay monotonically and can deteriorate significantly. This motivates us to propose an alternative approach below.

2.2 ESG-II. A modified Galerkin Approach

The standard Galerkin approach above is not restricted to spectral methods, and can be in principle used with other type of approximations. A special feature of the spectral methods is that, for smooth functions, their spectral expansion coefficients will decay exponentially fast. We shall construct a very good approximation of u_N^k, the solution of (2.6), based on this feature.

We define a projection operator $\Pi_N : X \to X_N$ by

$$a(\Pi_N v, w_N) = a(v, w_N), \quad \forall w_N \in X_N. \tag{2.12}$$

Assuming the solution u of (2.1) can be written as $u = u^* + \sum_{i=1}^{k} s_i \tilde{\psi}_i$, where u^* is the smooth part (compare with the singular terms $\tilde{\psi}_i$), which implies that

$$\Pi_N u^* = \Pi_N u - \sum_{i=1}^{k} s_i \Pi_N \tilde{\psi}_i. \tag{2.13}$$

Note that one can determine $\Pi_N u$ from

$$a(\Pi_N u, v_N) = a(u, v_N) = (f, v_N), \quad \forall v_N \in X_N, \tag{2.14}$$

and $\Pi_N \tilde{\psi}_i$ from

$$a(\Pi_N \tilde{\psi}_i, v_N) = a(\tilde{\psi}_i, v_N), \quad \forall v_N \in X_N,\ i = 1, 2, \ldots, k. \tag{2.15}$$

Now expanding the above in $\{\phi_j\}$, the basis functions of X_N, i.e.,

$$\Pi_N u^* = \sum_{j=1}^{N} u_j^* \phi_j;\ \Pi_N u = \sum_{j=1}^{N} u_j \phi_j;\ \Pi_N \tilde{\psi}_i = \sum_{j=1}^{N} \psi_{ij} \phi_j,\ i = 1, 2, \ldots, k,$$

we find

$$u_j^* = u_j - \sum_{i=1}^{k} s_i \psi_{ij},\ j = 1, 2, \ldots, N. \tag{2.16}$$

Since u^* is smooth, we know that u_j^* will be very close to zero for j sufficiently large. Hence, we can approximate its last k coefficients by zero, leading to

$$\sum_{i=1}^{k} \tilde{s}_i \psi_{ij} = u_j, \;\; j = N-k+1, N-k+2, \ldots, N, \tag{2.17}$$

where $\tilde{s}_i$ is an approximation of s_i $(i = 1, 2 \ldots, k)$. We can obtain $\{\tilde{s}_i\}$ by solving the above $k \times k$ linear system. With $\{\tilde{s}_i\}$ in hand, we look for a new approximation to u_N^k, the solution of (2.3), in the form of

$$\tilde{u}_N^k = \tilde{u}_N + \sum_{i=1}^{k} \tilde{s}_i \tilde{\psi}_i \quad \text{with} \;\; \tilde{u}_N \in X_N, \tag{2.18}$$

such that

$$a(\tilde{u}_N^k, v_N) =< f, v_N >, \quad \forall\, v_N \in X_N, \tag{2.19}$$

which leads to

$$a(\tilde{u}_N, v_N) =< f, v_N > - \sum_{i=1}^{k} \tilde{s}_i a(\tilde{\psi}_i, v_N) = a(\Pi_N u, v_N) - \sum_{i=1}^{k} \tilde{s}_i a(\Pi_N \tilde{\psi}_i, v_N).$$

Thanks to (2.2), we derive from the above that

$$\tilde{u}_N = \Pi_N u - \sum_{i=1}^{k} \tilde{s}_i \Pi_N \tilde{\psi}_i.$$

Finally, we obtain from the above and (2.18) that

$$\tilde{u}_N^k = \Pi_N u + \sum_{i=1}^{k} \tilde{s}_i (\tilde{\psi}_i - \Pi_N \tilde{\psi}_i). \tag{2.20}$$

To summarize, the following steps are needed for the modified Galerkin approach:

- Step 1: Determine $\Pi_N u$ and $\Pi_N \tilde{\psi}_i$ from (2.14) and (2.15), respectively.
- Step 2: Determine $\{\tilde{s}_i\}$ by solving the $k \times k$ linear system in (2.17).
- Step 3: Obtain the final approximation $\tilde{u}_N^k$ using (2.20).

Hence, the numerical implementation of the modified Galerkin approach is simpler and with less computational efforts than the standard Galerkin approach. Indeed, we do not need to compute $\tilde{\mathbf{f}}^s$, $\mathbf{C}$ and $\mathbf{D}$ in (2.9).

In general the linear system in (2.17) is still very ill-conditioned. However, we can now apply an oversampling procedure (see [1, Sec. 6] and references therein) to (2.17) to reduce the effect of ill-conditioning. More precisely, we compute m by k matrix $\mathbf{G}_{mk} = (\psi_{ij})$ with $m > k$, and determine the coefficients vector $\mathbf{S}_k = [\tilde{s}_1\ \tilde{s}_2\ \ldots\ \tilde{s}_k]^T$ by multiplying the generalized inverse matrix $(\mathbf{G}_{mk}^{\epsilon})^{\dagger}$ to truncated coefficients vector $\mathbf{U}_m = [u_{N-m+1}\ u_{N-m+2}\ \ldots\ u_N]^T$, namely,

$$\mathbf{S}_k = (\mathbf{G}_{mk}^{\epsilon})^{\dagger} \mathbf{U}_m$$

where $\mathbf{G}_{mk}^{\epsilon}$ is obtained by discarding all its singular values of $\mathbf{G}_{mk}$ below a given tolerance ϵ. We report in the right of Fig. 1 the results obtained using this procedure , and observe that the effect of ill-conditioning is significantly reduced to ESG-I.

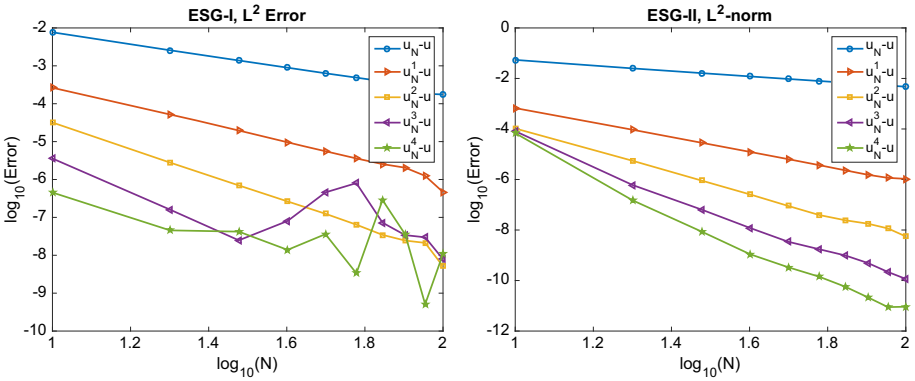

Fig. 1 Left: ESG-I, $\lambda = 1,\ s = 0.78$. Right: ESG-II, $\lambda = 1,\ s = 0.78$.

In order to demonstrate the difference between the ESG-I and ESG-II, we took (2.30) with $\lambda = 1$ and $s = 0.78$ as an example and plot in Fig. 1 the convergence rates by ESG-I and ESG-II (with $m - k = 10$ and $\epsilon = 10^{-10}$). We observe that both ESG-I and ESG-II lead to improved accuracy over the usual spectral-Galerkin method ($k = 0$), but as soon as $k > 2$, the results by ESG-I exhibit erratic behaviors due to the ill conditioning, but ESG-II still leads to improved results as N increases. As expected, ESG-II leads to algebraic convergence rate which increases as k increases.

2.3 Error Analysis for the Modified Galerkin Approach

Theorem 1 *Assuming that* $u = u^* + \sum_{i=1}^{k} s_i \tilde{\psi}_i$ *is the solution of* (2.1), *and* $\tilde{u}_N^k$ *be the numerical solution of ESG-II in* (2.20). *Then*

$$\|\tilde{u}_N^k - u\|_X \le \|\Pi_N u^* - u^*\|_X + \sum_{i=1}^{k} |s_i - \tilde{s}_i|\ \|\tilde{\psi}_i - \Pi_N \tilde{\psi}_i\|_X. \tag{2.21}$$

Proof We derive from (2.20) and $u = u^* + \sum_{i=1}^{k} s_i \tilde{\psi}_i$ that

$$\begin{aligned}
\tilde{u}_N^k - \Pi_N u^* - \sum_{i=1}^{k} s_i \tilde{\psi}_i &= \Pi_N u + \sum_{i=1}^{k} \tilde{s}_i (\tilde{\psi}_i - \Pi_N \tilde{\psi}_i) - \Pi_N u^* - \sum_{i=1}^{k} s_i \tilde{\psi}_i \\
&= \Pi_N (u - u^* - \sum_{i=1}^{k} s_i \tilde{\psi}_i) + \sum_{i=1}^{k} (\tilde{s}_i - s_i)(\tilde{\psi}_i - \Pi_N \tilde{\psi}_i) \qquad (2.22) \\
&= \sum_{i=1}^{k} (\tilde{s}_i - s_i)(\tilde{\psi}_i - \Pi_N \tilde{\psi}_i).
\end{aligned}$$

On the other hand,

$$\tilde{u}_N^k - u = \tilde{u}_N^k - u^* - \sum_{i=1}^{k} s_i \tilde{\psi}_i = \tilde{u}_N^k - \Pi_N u^* - \sum_{i=1}^{k} s_i \tilde{\psi}_i + \Pi_N u^* - u^*. \tag{2.23}$$

We then derive from the above two relations that

$$\|\tilde{u}_N^k - u\|_X \le \|\tilde{u}_N^k - \Pi_N u^* - \sum_{i=1}^{k} s_i \tilde{\psi}_i\|_X + \|\Pi_N u^* - u^*\|_X$$
$$\le \sum_{i=1}^{k} |\tilde{s}_i - s_i| \|\tilde{\psi}_i - \Pi_N \tilde{\psi}_i\|_X + \|\Pi_N u^* - u^*\|_X.$$

□

Remark 2.2 In the error estimate (2.21), the first term is small since u^* is assumed to be smooth, while in the second term, $\|\tilde{\psi}_i - \Pi_N \tilde{\psi}_i\|_X$ $(i = 1, 2, \ldots, k)$ are usually not small since $\{\tilde{\psi}_i\}$ are not smooth. However, $|\tilde{s}_i - s_i|$ $(i = 1, 2, \ldots, k)$ will be small since we can derive from (2.16) and (2.17) that

$$\sum_{i=1}^{k} (\tilde{s}_i - s_i)\psi_{ij} = u_j^*, \ \ j = N - k + 1, N - k + 2, \ldots, N, \tag{2.24}$$

and the fact that $\{u_j^*\}_{j=N-k+1}^{N}$ converge to zero fast as N increases since u^* is assumed to be smooth. □

Below and in subsequently sections, we shall demonstrate the effectiveness of ESG, particularly ESG-II, through several typical examples. In all examples, we shall follow the general procedure below:

- Formulate a weak formulation (2.1);
- Construct an usual spectral-Galerkin method in X_N (2.1);
- Determine the leading singular functions $\{\psi_j : j = 1, 2, \ldots, k\}$, apply the modified Gram-Schimdt process, and adjust them to $\{\tilde{\psi}_j : j = 1, 2, \ldots, k\}$ such that relevant homogeneous boundary conditions are satisfied;
- Setting $S_k = \text{span}\{\tilde{\psi}_j : j = 1, 2, \ldots, k\}$, and determine $u_N^k \in X_N \oplus S_k$ from (2.6) using ESG-I or ESG-II.

If not specified otherwise, ESG with the modified Galerkin approach, i.e. ESG-II, is used.

2.4 A 1-D Model Problem

We consider

$$\begin{cases} -u'' + u = f, \ \ x \in (-1, 1), \\ u(-1) = u(1) = 0, \end{cases} \tag{2.25}$$

with a prescribed exact solution

$$u = (1 + x)^{3/2}(1 - x) + (1 + x)^2 \log\big((1 + x)/2\big) + \sin(\pi x).$$

The related weak formulation is to find $u \in H_0^1(I) := \{v \in H^1(I) : v(\pm 1) = 0\}$ such that

$$a(u, v) := (u', v') + (u, v) = (f, v), \quad \forall v \in H_0^1(I). \tag{2.26}$$

Let P_N be the space of polynomials of degree less than or equal to N and $X_N = \{u \in P_N : u(\pm 1) = 0\}$. We shall use Jacobi polynomials to construct basis functions in many of the applications, we provide below some essential formulas (cf. [38]). Let $\alpha, \beta > -1$,

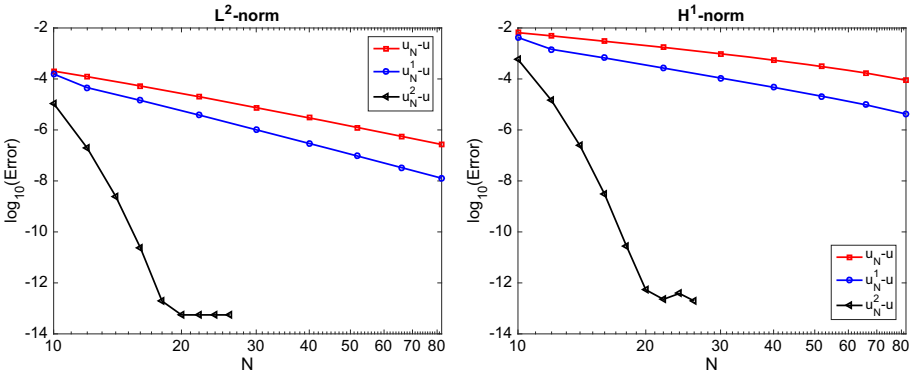

Fig. 2 Problem (2.25) with $u = (1+x)^{3/2}(1-x) + (1+x)^2 \log\big((1+x)/2\big) + \sin(\pi x)$

the classical Jacobi polynomials $J_n^{\alpha,\beta}(x)$ are orthogonal with respect to the weight function $w^{\alpha,\beta}(x) = (1-x)^\alpha(1+x)^\beta$ over $I := (-1, 1)$, i.e.

$$\int_I J_n^{\alpha,\beta}(x) J_m^{\alpha,\beta}(x) w^{\alpha,\beta}(x) \mathrm{d}x = \gamma_n^{\alpha,\beta} \delta_{mn}, \tag{2.27}$$

where

$$\gamma_n^{\alpha,\beta} = \frac{2^{\alpha+\beta+1}\Gamma(n+\alpha+1)\Gamma(n+\beta+1)}{(2n+\alpha+\beta+1)(n)!\Gamma(n+\alpha+\beta+1)}. \tag{2.28}$$

In particular, $L_n(x) = J_n^{0,0}(x)$ is the Legendre polynomial. It satisfies the following three-term recurrence relation:

$$\begin{cases} J_0^{\alpha,\beta}(x) = 1, \quad J_1^{\alpha,\beta}(x) = \frac{1}{2}(\alpha+\beta+2)x + \frac{1}{2}(\alpha-\beta), \\ J_{n+1}^{\alpha,\beta}(x) = (A_n^{\alpha,\beta}x - B_n^{\alpha,\beta})J_n^{\alpha,\beta}(x) - C_n^{\alpha,\beta} J_{n-1}^{\alpha,\beta}(x), \ n \geq 1, \end{cases} \tag{2.29}$$

where

$$\begin{aligned} A_n^{\alpha,\beta} &= \frac{(2n+\alpha+\beta+1)(2n+\alpha+\beta+2)}{2(n+1)(n+\alpha+\beta+1)}, \\ B_n^{\alpha,\beta} &= \frac{(\alpha^2-\beta^2)(2n+\alpha+\beta+1)}{2(n+1)(n+\alpha+\beta+1)(2n+\alpha+\beta)}, \\ C_n^{\alpha,\beta} &= \frac{(n+\alpha)(n+\beta)(2n+\alpha+\beta+2)}{(n+1)(n+\alpha+\beta+1)(2n+\alpha+\beta)}. \end{aligned}$$

We can then construct a set of suitable basis function for X_N using the Jacobi polynomials:

$$\phi_n(x) = (1-x^2)J_{n-1}^{1,1}(x), \ n = 1, \ldots, N-1.$$

Obviously, the two singular functions in the exact solution are

$$\psi_1(x) = (1+x)^{3/2}(1-x), \quad \psi_2(x) = (1+x)^2 \log\big((1+x)/2\big).$$

We can then apply the ESG to this problem.

We plot in Fig. 2 the errors of u_N^k, where $u_N^0 = u_N$ denotes the solution by the classical spectral-Galerkin method in X_N. The left figure shows the errors versus N in L^2 space, while the right figure shows the errors versus N in H^1 space. Due to the particular form of the exact solution, we achieve exponential convergence with $k = 2$.

2.5 A Singular Sturm–Liouville Problem

Consider the following second order Sturm–Liouville problem

$$\begin{cases} -u'' - \dfrac{\alpha}{y}u' + \lambda\, u = 0, \quad y \in \mathbb{R}^+ := (0,\infty), \\ u(0) = 1, \quad \lim\limits_{y\to\infty} u(y) = 0. \end{cases} \tag{2.30}$$

where $\lambda > 0$ and $\alpha = 1 - 2s$, $s \in (0, 1)$. We note that the related eigenvalue problem plays an important role in the numerical solution of fractional Laplacian equations by using the Caffarelli–Silvestre extension [8,27].

Setting $v = u - e^{-y/2}$, we can rewrite (2.30) as

$$\begin{cases} -(y^\alpha v')' + y^\alpha \lambda\, v = f, \quad y \in \mathbb{R}^+ := (0,\infty), \\ v(0) = 0, \quad \lim\limits_{y\to\infty} v(y) = 0, \end{cases} \tag{2.31}$$

where $f(y) = y^\alpha e^{-y/2}(\frac{1}{4} - \lambda - \frac{\alpha}{2y})$. Let $X = \{v : \int_0^\infty y^\alpha[(v')^2 + v^2]dy < \infty\}$. Thus, a weak formulation for the above is: Find $v \in X$ such that

$$a(v, w) := \int_0^\infty y^\alpha (v'\, w' + v\, w)\, \mathrm{d}y = \int_0^\infty f\, w\, dy, \quad \forall w \in X. \tag{2.32}$$

Let $L_n^{(\alpha)}(y)$ be the generalized Laguerre polynomials (cf. [34, Chapter 7]), a proper choice for X_N is

$$X_N := \mathrm{span}\{L_n^{(\alpha)}(y)e^{-y/2} : n = 0, 1, \ldots, N\}.$$

Then, the Laguerre spectral-Galerkin method for (2.32) is: Find $v_N \in X_N$ such that

$$a(v_N, w_N) = \int_0^\infty f\, w_N\, \mathrm{d}y, \quad \forall w_N \in X_N. \tag{2.33}$$

Singular Functions Due to the singular coefficient $1/y$ in the above solution, its solution is weak singular near $y = 0$. So we need to first derive its singular expansion. It can be shown [10, Proposition 2.1] that the exact solution is

$$u(y) = \begin{cases} e^{-\sqrt{\lambda}y}, & s = \dfrac{1}{2}; \\ c_s(\sqrt{\lambda}y)^s K_s(\sqrt{\lambda}y), & s \in (0,1)/\{\frac{1}{2}\}, \end{cases} \tag{2.34}$$

where K_s is the modified Bessel function

$$K_s(z) := \frac{s}{2}\frac{I_{-s}(z) - I_s(z)}{\sin(s\pi)} \quad \text{with} \quad I_s(z) := \sum_{j=0}^\infty \frac{1}{j!\Gamma(j+1+\alpha)}\Big(\frac{z}{2}\Big)^{2j+s}.$$

More precisely, for $s \in (0, 1)/\{\frac{1}{2}\}$, we have

$$u(y) = \frac{2^{1-s}}{\Gamma(s)}(\sqrt{\lambda}y)^s K_s(\sqrt{\lambda}y) = \frac{s2^{1-s}}{2\Gamma(s)\sin(s\pi)}\sum_{j=0}^\infty \frac{(\sqrt{\lambda}y)^{2j} - (\sqrt{\lambda}y)^{2j+2s}}{2^{2j+s}j!\Gamma(j+2-2s)},$$

which consists of a smooth part and a non-smooth part due to the factor y^{2s}.

It can be deduced from the above explicit expression that

$$\lim_{y\to 0} y^\alpha \psi'(y) = -d_s\lambda^s, \quad d_s := 2^{1-2s}\frac{\Gamma(1-s)}{\Gamma(s)}.$$

Then by the relation

$$\int_\Lambda y^\alpha[-u''(y)-\frac{\alpha}{y}u'(y)]v(y)\mathrm{d}y=\int_\Lambda -\big(y^\alpha u'(y)\big)'v(y)\mathrm{d}y=\big(y^\alpha u',v'\big)-d_s\lambda^s v(0),$$

A weak formulation for (2.31) is: find $u\in H^1_{y^\alpha}(\mathbb{R}^+):=\{w\in L^2_{y^\alpha}(\mathbb{R}^+):\ w'\in L^2_{y^\alpha}(\mathbb{R}^+)\}$

$$\big(y^\alpha u',v'\big)+\lambda\big(y^\alpha u,v\big)=d_s\lambda^s v(0),\quad v\in H^1_{y^\alpha}(\mathbb{R}^+).$$

However, we can not choose directly $\psi_i(y)=y^{2(i-1)+2s}$ since it behaves badly as $y\to\infty$. As in X_N, it appears that we should choose $\psi_i(y)=y^{2(i-1)+2s}e^{-y/2}$, but numerical results using these singular functions do not converge well as expected. The main reason is that, near $y=0$, we have

$$e^{-y/2}=1-y/2+y^2/8+\cdots$$

so near $y=0$,

$$\psi_1(y)=y^{2s}e^{-y/2}=y^{2s}-1/2y^{1+2s}+\cdots$$

includes the term y^{1+2s} which is not in the singular part of the solution, nor in any other $\psi_i(y)$ with $i\geq 2$. Therefore, we should set $\psi_i(y)=y^{i-1+2s}e^{-y/2}$ so that the unwanted terms like y^{1+2s} can be eliminated with proper linear combination of $\{\psi_i(y)\}$. Denote $X_N^k=X_N\oplus\{\psi_i:i=1,2,\ldots,k\}$. Then, we can apply the ESG to (2.5). The numerical results for this example are reported in Fig. 1.

3 Poisson Equations with Weakly Singular Solutions

We consider in this section several benchmark Poisson equations for which the solution includes weakly singular terms. We shall first determine forms of the first few singular terms and then apply the ESG to solve them.

3.1 Poisson Equation in a Rectangular Domain

Consider

$$\begin{cases}-\Delta u=f,\quad (x,y)\in\Omega:=(-1,1)^2,\\ u|_{\partial\Omega}=0.\end{cases}\tag{3.1}$$

Due to the corners in the domain, the solution will include weakly singular terms.

The weak formulation for (3.1) is: find $u\in H^1_0(\Omega)$ such that

$$(\nabla u,\nabla v)=(f,v),\quad v\in H^1_0(\Omega).\tag{3.2}$$

Let $X_N=\{v\in P_N\times P_N:v|_{\partial\Omega}=0\}$. Then the usual spectral-Galerkin method is: Find $u_N\in X_N$ such that

$$(\nabla u_N,\nabla v)=(f,v),\quad v\in X_N.\tag{3.3}$$

Let $\phi_k(z)=(1-z^2)J^{1,1}_{k-1}(z)$, then $X_N=\mathrm{span}\{\phi_k(x)\phi_j(y):1\leq k,j\leq N-1\}$. Using this basis function, the linear system associated with (3.3) can be efficiently solved by using the matrix diagonalization method [32]. We plot in Fig. 3 the error u_N-u with $N=12$ and $f=1$. Since no exact solution is available, we take u_N with $N=100$ as the reference

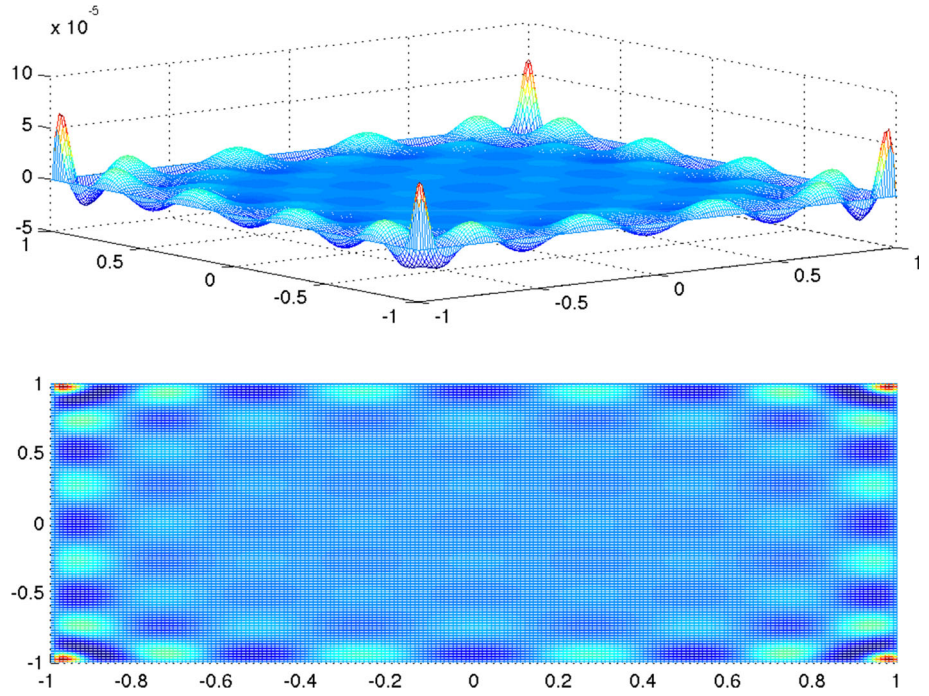

Fig. 3 Error by taking $N = 12$ and $f \equiv 1$

solution. We observe large errors near the four corners due to the corner singularity of the solution.

Singular Functions The nature of singularity for the Poisson equation is well known [17]. For the readers' convenience, we provide a derivation here which is suitable for our purpose. We start with the special case $f \equiv 1$. In this case, the problem (3.1) is equivalent to

$$\begin{cases} -\Delta w = 0, & (x, y) \in \Omega, \\ w|_{\partial\Omega} = \frac{1}{2}x^2, \end{cases} \tag{3.4}$$

where $w = u + \frac{1}{2}x^2$. We now follow the procedure in [22]. Near the point $(1, 1)$, the boundary condition can be rewritten by polar coordinate as

$$w(1, y) = \frac{1}{2}, \quad w(x, 1) = \frac{1}{2}x^2 = \frac{1}{2} - r - \frac{1}{2}r^2 \tag{3.5}$$

where

$$r(x, y) = \sqrt{(1 - x)^2 + (1 - y)^2}, \quad \theta(x, y) = \arctan(\frac{1 - x}{1 - y}).$$

We can then derive from [22, (2.36)] that the singular term takes the form

$$s(x, y) = \frac{1}{2} - \frac{1}{\pi}r^2\big(\ln r \ \sin(2\theta) + \theta\cos(2\theta)\big) - r\cos(\theta) + \frac{1}{2}r^2\cos(2\theta). \tag{3.6}$$

Similarly, we can deduce that the singular term near the points $(\pm 1, \pm 1)$ are $s(\pm x, \pm y)$, respectively.

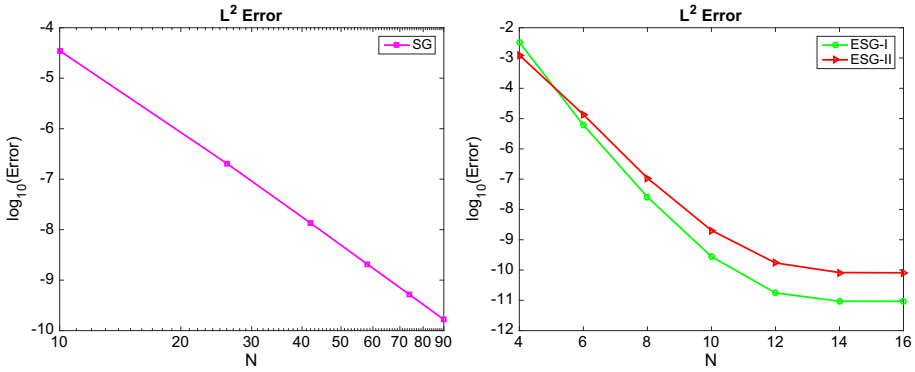

Fig. 4 Left: SG, right: ESG

For a general function $f(x, y) \in C(\bar{\Omega})$, one can show with a similar procedure that the singular term near $(1, 1)$ is $f(1, 1)s(x, y)$. Hence, summing up the four singular functions at the four corners, we obtain the singular function for the problem (3.1)

$$S(x, y) = f(1, 1)s(x, y)+f(-1, 1)s(-x, y)+f(1, -1)s(x, -y)+f(-1, -1)s(-x, -y). \tag{3.7}$$

One readily verified that $\Delta \mathcal{S} = 0$.

Note that the singular term $S(x, y)$ does not satisfy the homogeneous Dirichlet boundary condition, but we can follow the procedure in [32, subsection 4.2] to homogenize the boundary boundary condition, i.e., we can find $\phi_N \in P_N \times P_N$ such that $\phi_N(x, y)|_{\Sigma_N} = S(x, y)|_{\Sigma_N}$ where Σ_N is the spectral-collocation points at $\partial\Omega$. We set $\psi(x, y) = S(x, y) - \phi_N(x, y)$ and $X_N^1 = X_N \oplus \{\psi\}$. With the above preparations, we can then apply the ESG to (3.2).

As an example, we take $f(x, y) = e^{x+y}$ and compute approximate solutions by using the usual spectral-Galerkin (SG) method, ESG-I and ESG-II. Since no exact solution is available, we take the result of ESG-I with $N = 100$ as the reference solution. In Fig. 4, we plot the convergence rates of SG on the left, and that of ESG-I and ESG-II on the right. We observe that the errors for the SG converges algebraically due to the corner singularity, but both ESG-I and ESG-II converge exponentially since the singular function is built in the approximation space. ESG-I leads to slightly better accuracy as ESG-II is in fact an approximation of ESG-I.

3.2 Poisson Equation on a Semicircle Domain

We consider the Poisson equation with mixed Dirichlet–Neumann boundary condition

$$\begin{cases} -\Delta u = f, & (\zeta, \eta) \in \Omega \subset \mathbb{R}^2, \\ u\big|_{\Gamma_D} = 0, & \dfrac{\partial u}{\partial \vec{n}}\Big|_{\Gamma_N} = 0, \end{cases} \tag{3.8}$$

where $\Gamma_D \cup \Gamma_N = \partial\Omega$. This problem has been considered in many previous work, cf. [21,25,35]. we first derive a weak formulation which is suitable for spectral approximation.

Let (r, θ) be the polar coordinates with $(\zeta, \eta) = (r\cos\theta, r\sin\theta)$. Then, the problem (3.8) is transformed to

$$-\frac{1}{r}\partial_r(r\partial_r u) - \frac{1}{r^2}\partial_\theta^2 u = f, \quad (r, \theta) \in (0, 1) \times (0, \pi), \tag{3.9}$$

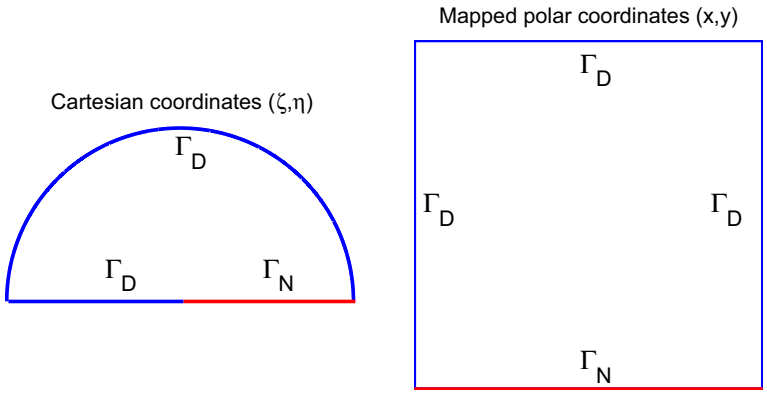

Fig. 5 Original domain in Cartesian coordinates (ζ, η) and mapped domain in polar coordinates (x, y)

with the boundary conditions

$$u(0,\theta) = u(1,\theta) = 0, \quad \partial_\theta u(r,0) = u(r,\pi) = 0. \tag{3.10}$$

For the sake of simplicity, we still use u, f and Ω to denote the transformed functions and domain. the original domain is transformed onto the mapped domain in polar coordinates, cf. Fig. 5.

In order to use Jacobi polynomials which are defined on the interval $[-1, 1]$, we make another affine mapping

$$x = 2r - 1, \quad y = 2\theta/\pi - 1. \tag{3.11}$$

The original problem (3.8) is equivalent to

$$\begin{cases} -\partial_x((1+x)\partial_x u) - \dfrac{4}{\pi^2}\dfrac{1}{1+x}\partial_y^2 u = \dfrac{1+x}{4} f, \quad (x,y) \in \Omega = (-1,1)^2, \\ u(\pm 1, y) = 0, \quad \partial_y u(x,-1) = 0, \quad u(x,1) = 0. \end{cases} \tag{3.12}$$

The weak formulation for (3.12) is: find $u \in H_b^1(\Omega)$ such that

$$a(u,v) = F(v), \quad \forall v \in H_b^1(\Omega). \tag{3.13}$$

where

$$H_b^1(\Omega) := \{u \in H^1(\Omega) : \ u(\pm 1, y) = 0, \ u(x,1) = 0\}$$

and

$$a(u,v) := \big((1+x)\partial_x u, \partial_x v\big) + \frac{4}{\pi^2}\Big(\frac{1}{1+x}\partial_y u, \partial_y v\Big), \quad F(v) := \Big(\frac{(1+x)}{4} f, v\Big).$$

Next, we describe the spectral-Galerkin method. Let us denote

$$\phi_i(x) = (1-x^2)J_i^{1,1}(x), \quad \psi_j(y) = (1-y)J_j^{1,0}(y). \tag{3.14}$$

Then $\phi_i(x)\psi_j(y)$ satisfies the boundary conditions in (3.12). Let $X_N = \text{span}\{\phi_i(x)\psi_j(y)\}_{i,j=0}^{N-2}$. The spectral Galerkin method for (3.13) is: find $u_N \in X_N$ s.t.

$$a(u_N, v_N) = F(v_N), \quad \forall v_N \in X_N. \tag{3.15}$$

A fast algorithm can be developed as in [32] for the above system.

Singular functions at the origin. Since the singularity at the two corners of the semicircle is much weaker than that at the origin caused by the mismatch of boundary conditions, we shall concentrate on the latter.

It is well known [21,25] that the general admissible solution of the Laplace equation i.e. $f = 0$ in (3.9), in polar coordinates are

$$u^L(r,\theta) = r^\alpha\big(a\cos(\alpha\theta) + b\sin(\alpha\theta)\big),$$

where $\alpha > 0$, a, b are constants. The Neumann boundary condition at Γ_N implies that the general solutions of the Laplacian equation can be expanded as

$$u^L(r,\theta) = \sum_{n=0}^{\infty} c_n r^{\alpha_n}\cos(\alpha_n\theta), \quad \alpha_n = n + \frac{1}{2} \tag{3.16}$$

which automatically satisfies

$$u^L(0,\theta) = 0, \quad \partial_\theta u^L(r,0) = u^L(r,\pi) = 0.$$

Hence, the solution of Poisson equation (3.9) with mixed boundary condition (3.10) can be separated into

$$u(r,\theta) = u^L(r,\theta) + u^R(r,\theta),$$

where the regular part satisfies the Poisson equation (3.9) and with the boundary condition

$$u^R(0,\theta) = 0, \quad u^R(1,\theta) = -u^L(1,\theta), \quad \partial_\theta u^R(r,0) = u^R(r,\pi) = 0.$$

Therefore, we can use as the singular functions

$$\psi_n(x,y) := [(1+x)^{\alpha_n} - 2^{\alpha_n-1}(1+x)]\cos\left(\frac{\pi}{2}\alpha_n(1+y)\right), \quad \alpha_n = n + \frac{1}{2},\ n = 0,1,\ldots \tag{3.17}$$

which also satisfy the required boundary conditions. Setting

$$S_k := \text{span}\{\psi_0,\ \psi_1,\ \ldots,\ \psi_{k-1}\},$$

we can then apply ESG to this problem.

As examples, we solve the Poisson equation (3.8) with $f = \sin(\pi x)\sin(\pi y)$ and $f = 1$. Since the exact solution is unknown, we used the result of ESG-II with a large $N = 100$, $k = 2$ as the reference solution. Figure 6 shows the convergence rate of SG and ESG-II. We observe that with each additional singular term, the convergence rate is increased by two. This is due to the clustering of the collocation points near boundaries for the spectral method, which can lead to twice the normal convergence rate for problems with corner singularities. This phenomenon is also observed for other numerical examples presented below. For the case of $f = 1$, adding more singular functions near origin will not improve further as the next leading singular function, after $\psi_2(x,y)$, is the one at the corner $(-1,0)$.

3.3 Poisson Equation on a Circular Domain with a Slit

We consider

$$\begin{cases} -\Delta u = f, & \text{in } \Omega = \{(\zeta,\eta) : \zeta^2 + \eta^2 < 1\}, \\ u\big|_{\Gamma_D} = 0, & \dfrac{\partial u}{\partial \vec{n}}\Big|_{\Gamma_N} = 0, \end{cases} \tag{3.18}$$

where $\Gamma_D \cup \Gamma_N = \partial\Omega$, cf. the left of Fig. 7. This is a benchmark problem considered in [4].

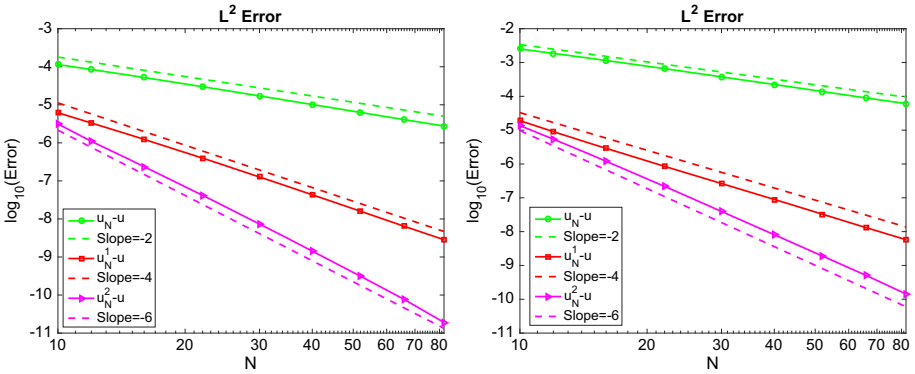

Fig. 6 ESG for (3.8), left: $f = \sin(\pi x)\sin(\pi y)$. Right: $f \equiv 1$

Note that while Ω is a circle, the solution in polar coordinates is not periodic in the spanwise θ-direction so we can not use a Fourier spectral expansion in the θ-direction.

Similarly as in the semi-circle case, with a polar transform $(\zeta, \eta) = (r\cos\theta, r\sin\theta)$ followed by an affine mapping

$$x = 2r - 1, \quad y = 1 - \theta/\pi. \tag{3.19}$$

The equation (3.18) is trasformed to

$$\begin{cases} -\partial_x((1+x)\partial_x u) - \dfrac{1}{\pi^2}\dfrac{1}{1+x}\partial_y^2 u = \dfrac{1+x}{4} f, \quad (x, y) \in (-1, 1)^2, \\ u(\pm 1, y) = 0, \quad \partial_y u(x, -1) = 0, \quad u(x, 1) = 0. \end{cases} \tag{3.20}$$

Then, the weak formulation and an efficient spectral-Galerkin method can be formulated as in the semi-circle case. Note that the spectral-Galerkin method in [33] based on the Fourier expansion in the θ-direction can not be used here due to the fact that the solution to (3.18) is no longer periodic in the θ-direction.

Thanks to [4, (4a)], the singular terms about the origin can be expressed as

$$s_n = r^{\beta_n}\sin(\beta_n\theta), \quad \beta_n = \frac{2n-1}{4}, \quad n = 1, 2, \ldots. \tag{3.21}$$

Now we have all the ingredients to apply ESG to (3.20). We plot the numerical result with $f \equiv 1$ by ESG-II in the right of the Fig. 7 where we take the result of ESG-II with $N = 150$ as the reference solution.

3.4 A Nonlinear Problem

As the last example of this section, we consider a nonlinear problem

$$\begin{cases} F(u) := -\Delta u + u^3 - u - f = 0 \quad \text{in } \Omega := (-1, 1)^2; \\ u|_{\partial\Omega} = 0. \end{cases} \tag{3.22}$$

Using the Newton iterative method [36], we are led to solve, at each iteration

$$\begin{cases} -\Delta w + (3u_k^2 - 1)w = -\Delta u_k + (u_k^3 - u_k) - f, \quad w|_{\partial\Omega} = 0; \\ u_{k+1} = u_k - w. \end{cases} \tag{3.23}$$

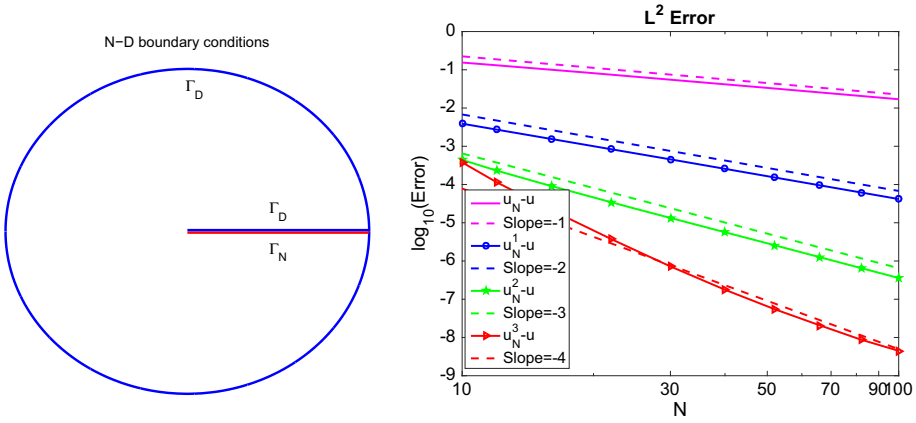

Fig. 7 Left: circle domain, right: $f \equiv 1$

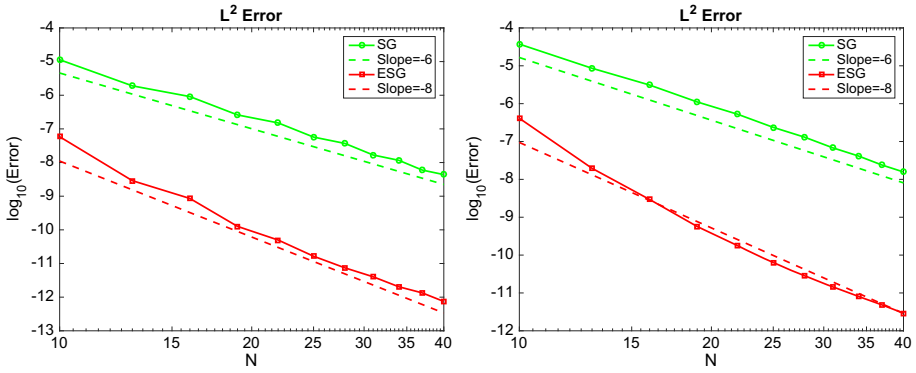

Fig. 8 A nonlinear example: Left: $f \equiv 1$, right: $f = e^{x+y}$

Similar to the Poisson equation on the square domain considered at the beginning of this section, the spectral-Galerkin method for (3.23) is to find $w_N \in X_N = \{v \in P_N \times P_N : v|_{\partial\Omega} = 0\}$ such that

$$\begin{cases} (\nabla w_N, \nabla v_N) + ((3(u_N^k)^2 - 1)\, w_N, v_N) = (\nabla u_N^k, \nabla v_N) + ((u_N^k)^3 - u_N^k, v_N) - (f, v_N), \quad \forall v_N \in X_N, \\ u_N^{k+1} = u_N^k - w_N. \end{cases} \tag{3.24}$$

It is clear that the solution of the nonlinear problem still exhibits weak singularity at the corners. Due to the homogeneous boundary conditions, the influence of the nonlinear term u^3 to the leading singularity can be neglected so we can still take the singular term (3.7) of the Poisson equation as the leading singular term for the nonlinear term.

We plot in Fig. 8 convergence rates by SG and ESG with $f = 1$ and $f = e^{x+y}$, and taking the result of ESG with $N = 100$ as the reference solution. We observe that in both cases, ESG improves significantly over SG.

4 Fractional Differential Equation

We consider in this section the following fractional differential equation

$$\begin{cases} -{}_{-1}\mathrm{D}_x^{\mu} u + C\, u = f, \quad \mu = 2s \in (1,2), \\ u(-1) = u(1) = 0. \end{cases} \tag{4.1}$$

where $C > 0$ and ${}_{-1}\mathrm{D}_x^{\mu}$ is the left Riemann–Liouville fractional derivative of order μ defined below.

For $a, b \in \mathbb{R}$ and $\rho \in \mathbb{R}^+$, the left and right fractional integrals are respectively defined as (see e.g., [28,29]):

$${}_a\mathrm{I}_x^{\rho} v(x) = \frac{1}{\Gamma(\rho)} \int_a^x \frac{v(y)}{(x-y)^{1-\rho}} dy, \quad {}_x\mathrm{I}_b^{\rho} v(x) = \frac{1}{\Gamma(\rho)} \int_x^b \frac{v(y)}{(y-x)^{1-\rho}} dy, \quad x \in (a,b). \tag{4.2}$$

Then, the left and right Riemann-Liouville fractional derivatives are defined by

$${}_a\mathrm{D}_x^{s} v(x) = \frac{d^k}{dx^k} \{ {}_a\mathrm{I}_x^{k-s} v(x) \}, \quad {}_x\mathrm{D}_b^{s} v(x) = (-1)^k \frac{d^k}{dx^k} \{ {}_x\mathrm{I}_b^{k-s} v(x) \}, \tag{4.3}$$

where the real number $s \in [k-1, k)$ with $k \in \mathbb{N}$.

As shown in [13,20], for any $u, v \in X := H_0^s$, we have

$$({}_{-1}\mathrm{D}_x^{2s} u, v) = ({}_{-1}\mathrm{D}_x^{s} u, {}_x\mathrm{D}_1^{s} v).$$

Hence, a weak formulation for (4.3) is: Find $u \in X$ such that

$$a(u,v) := -({}_{-1}\mathrm{D}_x^{s} u, {}_x\mathrm{D}_1^{s} v) + C\,(u,v) = (f,v) \quad \forall v \in X.$$

Then, the spectral-Galerkin approximation for the above is: Find $u_N \in X_N := \{u \in P_N : u(\pm 1) = 0\}$ such that

$$a(u_N, v_N) = (f, v_N), \quad v_N \in X_N. \tag{4.4}$$

As before, we choose as basis functions of X_N,

$$\phi_n(x) := (1-x^2) J_n^{1,1}(x), \quad n = 0, 1, \ldots. \tag{4.5}$$

Then, one can verify that (c.f. [11, eqs. (2.23)–(2.26) and Lemma 2.5])

$$\begin{aligned} {}_{-1}\mathrm{D}_x^{r} \{\phi_n(x)\} &= -2(n+1) \frac{\Gamma(n+2)}{\Gamma(n+3-r)} (1+x)^{1-r} J_{n+1}^{r-1,1-r}(x), \\ {}_{x}\mathrm{D}_1^{r} \{\phi_n(x)\} &= 2(n+1) \frac{\Gamma(n+2)}{\Gamma(n+3-r)} (1-x)^{1-r} J_{n+1}^{1-r,r-1}(x). \end{aligned} \tag{4.6}$$

Hence, one can easily compute the stiffness and mass matrices.

4.1 Singular functions

It is well known that the solution of the problem (4.1) is usually weakly singular at the left endpoint $x = -1$ even when f is smooth. We first determine singular solutions associated to this problem. We recall the following formula (cf. [12,28,29]):

$${}_{-1}\mathrm{D}_x^{\beta} (1+x)^{\alpha} = \begin{cases} \frac{\Gamma(\alpha+1)}{\Gamma(\alpha-\beta+1)} (1+x)^{\alpha-\beta}, & \alpha - \beta > -1, \\ 0, & \beta - \alpha = 1, 2, \ldots. \end{cases} \tag{4.7}$$

We shall assume that $f(x)$ has a Taylor expansion near $x = -1$, namely:

$$f(x) = \sum_{i=0}^{\infty} \hat{f}_i (1+x)^i.$$

For fixed $i \geq 0$, let us first consider (4.1) with $f = (1+x)^i$. Due to (4.7), it is natural to look for solution of (4.1) near $x = -1$ in the form

$$u(x) = \sum_{p=0}^{\infty} c_p (1+x)^{\lambda_p}, \quad 0 < \lambda_p < \lambda_{p+1}. \tag{4.8}$$

Plug the above in (4.1) with $f = (1+x)^i$, we obtain

$$-c_0 \frac{\Gamma(\lambda_0+1)}{\Gamma(\lambda_0-\mu+1)}(1+x)^{\lambda_0-\mu} - \sum_{p=0}^{\infty} \left\{ c_{p+1} \frac{\Gamma(\lambda_{p+1}+1)}{\Gamma(\lambda_{p+1}-\mu+1)}(1+x)^{\lambda_{p+1}-\mu} - C c_p (1+x)^{\lambda_p} \right\} = (1+x)^i.$$

We derive from the above that we must have

$$\lambda_0 - \mu = i, \quad \lambda_{p+1} - \mu = \lambda_p, \ p \geq 0,$$

which implies $\lambda_p = i + (p+1)\mu, \ p \geq 0$, for all $i \geq 0$. Summing up for all i, we find that near $x = -1$, u should take the form

$$u(x) = \sum_{i,j=0}^{\infty} \hat{u}_{ij} (1+x)^{i+(j+1)\mu}.$$

On the other hand, we also derive from (4.7) that

$$-_{-1}\mathrm{D}_x^{\mu}(1+x)^{\mu-1} = 0.$$

Hence, we must add the term $(1+x)^{\mu-1}$ to the singular expansion above, leading to the final form

$$u(x) = \sum_{i,j=0}^{\infty} \hat{u}_{ij} (1+x)^{i-1+(j+1)\mu}. \tag{4.9}$$

Remark 4.1 Another way to derive the singular expansion for fractional PDEs is to use the so called Mittag-Leffler functions. For example, it can be shown that solution to the following Caputo fractional differential equation

$${}_0^C\mathrm{D}_t^{\nu} y(t) + \mathcal{K} y(t) = f(t), \quad y(0) = y_0, \qquad t > 0, \ \nu \in (0,1), \ \mathcal{K} \in \mathbb{R}. \tag{4.10}$$

can be expressed as [15] (see also [12, (7.3)])

$$y(t) = y_0 \, E_{\nu,1}(-\mathcal{K} t^{\nu}) + \int_0^t (t-\tau)^{\nu-1} E_{\nu,\nu}[-\mathcal{K}(t-\tau)^{\nu}] f(\tau) \mathrm{d}\tau, \tag{4.11}$$

where $E_{\nu,1}$ and $E_{\nu,\nu}$ are two kinds of specific Mittag-Leffler functions (See [18,19,28]).

Remark 4.2 Note that, instead of using $X_N = \{v \in P_N : v(\pm 1) = 0\}$, one can also use, as in [11], $\tilde{X}_N = \mathrm{span}\{{}^{-}J_k^{(-1,1-\mu)} : k = 1, \ldots, N\}$, where ${}^{-}J_k^{(-1,1-\mu)}$ are the so called generalized Jacobi functions defined in [11] (cf. also [39]). It leads exponential convergence if $C = 0$ in (4.1) but will not perform well if $C \neq 0$ since only the leading singular term $(1+x)^{\mu-1}$ is present in the basis functions $\{{}^{-}J_k^{(-1,1-\mu)}\}$.

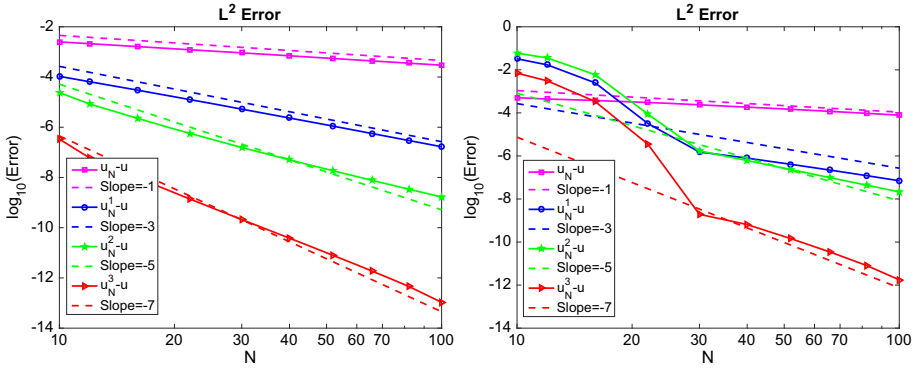

Fig. 9 Left: $C = 1$, $\mu = 1.3$, $f = e^x \sin(x)$, right: $C = 50$, $\mu = 1.3$, $f = e^x \sin(x)$

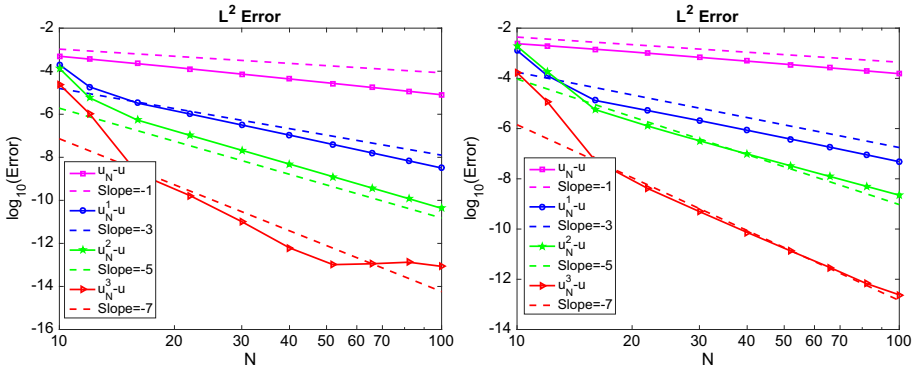

Fig. 10 Left: $C = 10$, $\mu = 1.7$, $f = e^x$, right: $C = 10$, $\mu = 1.41$, $f = e^x$

4.2 Enriched Spectral-Galerkin Method and Numerical Results

We denote the k leading singular terms in (4.9) by $\{\psi_{r_m} : m = 1, \ldots, k\}$ with $r_m = i - 1 + (j + 1)\mu$ increasing. Setting

$$S_k = span\{\psi_{r_m} : m = 1, \ldots, k\}, \tag{4.12}$$

the enriched spectral-Galerkin method for problem (4.1) is: find $u_N^k \in X_N^k := X_N \oplus S_k$ such that

$$a(u_N^k, v) = (f, v), \quad \forall v \in X_N^k. \tag{4.13}$$

Since the singular terms are indeed Jacobi weight functions, additional entries in the mass and stiffness matrices related to S_k can be straightforwardly computed by a suitable Jacobi Gauss quadrature formula.

We now present several numerical tests to show the efficiency and accuracy of ESG. In Fig. 9, we plot the convergence rate of $f = e^x \sin(x)$ with $C = 1$, $\mu = 1.3$ and $C = 50$, $\mu = 1.3$ to demonstrate that the method is robust with respect to constant C. We take the result u_N^3, $N = 150$ as the reference solution, and plot in Fig. 10 for the convergence rate of $f = e^x$ with $C = 10$, $\mu = 1.7$ and $C = 10$, $\mu = 1.41$ to show its effectiveness with different μ.

5 Conclusion

We developed in this paper enriched spectral-Galerkin methods (ESG) for solving PDEs with weakly singular solutions. While the general idea of ESG is very simple—adding leading singular functions to the usual spectral approximation space, one has to overcome several obstacles to efficiently and accurately implement this in practical situations. Successful implementations of ESG rely on three ingredients: (i) determine a few leading singular terms for the underlying problem; (ii) homogenize the boundary conditions for the singular functions and use the modified Gram–Schimdt process to orthogonalize them; and most importantly (iii) use ESG-II, which is based on a special property of the spectral methods, to approximate the solution in the enriched spectral space. The computational cost of ESG-II is essentially $k+1$ solvers, with k being the number of used leading singular terms, of the usual spectral-Galerkin method for which fast solvers are in general available. Theoretical estimates indicate that the accuracy of ESG can be as high as needed by increasing k, however, ill conditioning of the enriched spaces often prevents the use of a large number of singular functions. It is found that if we only add one or two singular functions, ESG-I and ESG-II lead to similar results. But if more than two singular functions are used, ESG-I often exhibits erratic behavior while ESG-II is much more stable.

We applied ESG to a variety of problems with weakly singular solutions, and showed that ESG is capable of producing significantly improved results over the usual spectral-Galerkin methods with adding only a few singular functions. Compared with other approaches often used in the context of spectral methods, such as singularity subtraction or Müntz method, ESG is easier to implement and more accurate than singularity subtraction, while it applies to a large class of problems than Müntz method.

References

1. Adcock, B., Huybrechs, D.: Frames and numerical approximation (2016). arXiv:1612.04464 [math.NA]
2. Auteri, F., Parolini, N., Quartapelle, L.: Numerical investigation on the stability of singular driven cavity flow. J. Comput. Phys. **183**(1), 1–25 (2002)
3. Babuška, I., Banerjee, U.: Stable generalized finite element method (SGFEM). Comput. Method Appl. M. **201**, 91–111 (2012)
4. Babuška, I., Miller, A.: The post–processing approach in the finite element method–Part 2: The calculation of stress intensity factors. Int. J. Numer. Meth. Eng. **20**(6), 1111–1129 (1984)
5. Björck, A., Paige, C.C.: Loss and recapture of orthogonality in the modified gram-schmidt algorithm. SIAM J. Matrix Anal. Appl. **13**(1), 176–190 (1992)
6. Botella, O., Peyret, R.: Computing singular solutions of the naviercstokes equations with the chebyshev collocation method. Int. J. Numer. Methods Fluids **36**, 125 (2001)
7. Boyd, J.P.: Chebyshev and Fourier Spectral Methods. Dover, New York (2001)
8. Caffarelli, L., Silvestre, L.: An extension problem related to the fractional laplacian. Comm. Partial Differ. Eq. **32**(8), 1245–1260 (2007)
9. Canuto, C., Hussaini, M.Y., Quarteroni, A., Zang, T.A.: Spectral Methods: Fundamentals in Single Domains. Springer, Berlin (2006)
10. Capella, A., Dávila, J., Dupaigne, L., Sire, Y.: Regularity of radial extremal solutions for some non-local semilinear equations. Commun. Part. Differ. Eq. **36**(8), 1353–1384 (2011)
11. Chen, S., Shen, J., Wang, L.L.: Generalized jacobi functions and their applications to fractional differential equations. Math. Comput. **85**(300), 1603–1638 (2016)
12. Diethelm, K.: The Analysis of Fractional Differential Equations. Lecture Notes in Math, vol. 2004. Springer, Berlin (2010)
13. Ervin, V.J., Roop, J.P.: Variational formulation for the stationary fractional advection dispersion equation. Numer. Methods Partial Differ. Equ. **22**(3), 558–576 (2006)

14. Fries, T.P., Belytschko, T.: The extended/generalized finite element method: an overview of the method and its applications. Int. J. Numer. Methods Eng. **84**(3), 253–304 (2010)
15. Gorenflo, R., Mainardi, F.: Fractional oscillations and Mittag-Leffler functions. Citeseer, Prineton (1996)
16. Gottlieb, D., Orszag, S.A.: Numerical Analysis of Spectral Methods: Theory and Applications. Number 26 in CBMS-NSF Regional Conference Series in Applied Mathematics. SIAM, Philadelphia (1977)
17. Grisvard, P.: Elliptic Problems in Nonsmooth Domains, vol. 69. SIAM, Philadelphia (2011)
18. Haubold, H.J., Mathai, A.M., Saxena, R.K.: Mittag-Leffler functions and their applications. J. Appl. Math. **2011**, 298628 (2011). https://doi.org/10.1155/2011/298628
19. Kilbas, A.A., Srivastava, H.M., Trujillo, J.J.: Theory and Applications of Fractional Differential Equations. Elsevier, Amsterdam (2006)
20. Li, X., Xu, C.: A space-time spectral method for the time fractional diffusion equation. SIAM J. Numer. Anal. **47**(3), 2108–2131 (2009)
21. Li, Z.C., Lu, T.T.: Singularities and treatments of elliptic boundary value problems. Math. Comput. Mod. **31**(8), 97–145 (2000)
22. Li, Z.C., Lu, T.T., Hu, H.Y., Cheng, A.H.: Particular solutions of laplace's equations on polygons and new models involving mild singularities. Eng. Anal. Bound. Elem. **29**(1), 59–75 (2005)
23. Mao, Z., Chen, S., Shen, J.: Efficient and accurate spectral method using generalized Jacobi functions for solving Riesz fractional differential equations. Appl. Numer. Math. **106**, 165–181 (2016)
24. Mao, Z., Karniadakis, G.E.: A spectral method (of exponential convergence) for singular solutions of the diffusion equation with general two-sided fractional derivative. SIAM J. Numer. Anal. **56**(1), 24–49 (2018)
25. Marin, L., Lesnic, D., Mantič, V.: Treatment of singularities in helmholtz-type equations using the boundary element method. J. Sound Vib. **278**(1), 39–62 (2004)
26. Morin, P., Nochetto, R., Siebert, K.G.: Convergence of adaptive finite element methods. SIAM Rev. **44**(4), 631–658 (2002)
27. Nochetto, R.H., Otárola, E., Salgado, A.J.: A pde approach to fractional diffusion in general domains: a priori error analysis. Found. Comput. Math. **15**(3), 733–791 (2014)
28. Podlubny, I.: Fractional Differential Equations, volume 198 of Mathematics in Science and Engineering. Academic Press Inc., San Diego, CA, (1999). An introduction to fractional derivatives, fractional differential equations, to methods of their solution and some of their applications
29. Samko, S.G., Kilbas, A.A., Maričev, O.I.: Fractional Integrals and Derivatives. Gordon and Breach Science Publ, Philadelphia (1993)
30. Schultz, W.W., Lee, N.Y., Boyd, J.P.: Chebyshev pseudospeetral method of viscous flows with corner singularities. J. Sci. Comput. **4**, 1–24 (1989)
31. Schumack, M.R., Schultz, W.W., Boyd, J.P.: Spectral method solution of the stokes equations on nonstaggered grids. J. Comput. Phys. **94**(1), 30–58 (1991)
32. Shen, J.: Efficient spectral-Galerkin method I. Direct solvers for second- and fourth-order equations by using Legendre polynomials. SIAM J. Sci. Comput. **15**(6), 1489–1505 (1994)
33. Shen, J.: Efficient spectral-Galerkin methods III. Polar and cylindrical geometries. SIAM J. Sci. Comput. **18**, 1583–1604 (1997)
34. Shen, J., Tang, T., Wang, L.L.: Spectral Methods: Algorithms, Analysis and Applications. Series in Computational Mathematics, vol. 41. Springer, Berlin (2011)
35. Shen, J., Wang, Y.: Müntz–Galerkin methods and applications to mixed Dirichlet–Neumann boundary value problems. SIAM J. Sci. Comput. **38**(4), A2357–A2381 (2016)
36. Sherman, A.H.: On newton-iterative methods for the solution of systems of nonlinear equations. SIAM J. Numer. Anal. **15**(4), 755–771 (1978)
37. Strang, G., Fix, G.J.: An Analysis of the Finite Element Method. Prentice-Hall Series in Automatic Computation. Prentice-Hall Inc, Englewood Cliffs (1973)
38. Szego, G.: Orthogonal Polynomials, vol. 23 of Amer. In: Math. Soc. Colloq. Publ., Amer. Math. Soc., Providence, RI (1975)
39. Zayernouri, M., Karniadakis, G.E.: Exponentially accurate spectral and spectral element methods for fractional ODEs. J. Comput. Phys. **257**(Part A), 460–480 (2014)